Corking and Uncorking a Catalytic Yolk–Shell Nanoreactor: Stable Gold Catalyst in Hollow Silica Nanosphere

ARTICLE *in* JOURNAL OF PHYSICAL CHEMISTRY LETTERS · NOVEMBER 2011

Impact Factor: 7.46 · DOI: 10.1021/jz201336h

5 AUTHORS, INCLUDING:

Si-Han Wu
Taipei Medical University
20 PUBLICATIONS **1,993** CITATIONS

SEE PROFILE

Chung-Yuan Mou
National Taiwan University
381 PUBLICATIONS **13,541** CITATIONS

SEE PROFILE

THE JOURNAL OF PHYSICAL CHEMISTRY Letters

LETTER

pubs.acs.org/JPCL

Corking and Uncorking a Catalytic Yolk-Shell Nanoreactor: Stable Gold Catalyst in Hollow Silica Nanosphere

Chen-Han Lin, Xiaoyan Liu, Si-Han Wu, Kao-Hsiang Liu, and Chung-Yuan Mou*

Department of Chemistry, National Taiwan University, Taipei, Taiwan 10617

Supporting Information

ABSTRACT: Silica templating of a water-in-oil (w/o) microemulsion system containing $HAuCl_4$ results in gold nanoparticles of sizes around 3 nm confined in hollow silica nanospheres. The size of the gold nanocatalyst is stable to high temperature calcination. Its catalytic activity toward CO oxidation is very stable after repeated use and long-time storage. The reaction can be controlled by a corking design based on capillary condensation of water vapor for corking the mesopores on the shell. At higher temperature or low water vapor pressure, pores open after vapor evaporation and water promotes the CO oxidation. The corking and uncorking mechanism of the yolk-shell type nanoreactor is reversible.

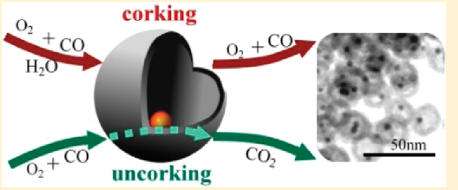

SECTION: Surfaces, Interfaces, Catalysis

Metal nanoparticles (NPs) exhibiting high activity, selectivity and stability play a key role in heterogeneous catalysis. There has been intense recent interest in developing nanostructured oxide-supported metal catalyst.[1−5] The purpose is to precisely control its particle size and enhance its thermal stability. This is important for application under realistic technical conditions. For low melting gold NPs, sintering can be serious either during high temperature pretreatment[5] or in reaction.[6] Most often, a combination of mesoporous structural compartmentization and stronger metal−support interactions are required so that metal NPs do not move easily on the nanostructured support. Examples are Au−CeO_2 mesoporous nanocomposites[7] and metal-layered double hydroxides (LDHs).[8] However, for weaker metal−support interactions such as Au−silica, most strategies against sintering did not work well at high temperature. Here, an encapsulation approach of metal NPs in hollow porous shells of inorganic materials with "rattle" type nanoreactors as catalysts would be most desirable.[9,10] Because of the one-particle−one-hollow-sphere confinement, sintering is excluded, and the encapsulated metal NP is stable at high temperature, either in pretreatment or in reaction.

Typically, these hollow particles are created by either of two approaches: sacrificing a portion of the hard-template particles or co-condensation during fabrication of hollow silica. However, the particle sizes of the encapsulated metal NPs (the yolk) are often too big, in tens of nanometers, to be active catalysts.[11,12] Thus, often only "easy" solution state reactions, such as catalytic reduction of nitrophenol, are demonstrated. The caztalytic performance of size-sensitive Au nanocatalysts (Au NP size ∼3 nm) in the benchmark reaction (CO oxidation) has not been reported. Moreover, the creation of porous shells in Au-containing yolk−shell structure may provide new opportunities for designing smart gated catalytical nanoreactors.

Recently, we reported hollow silica nanospheres (HSNs; sub-100 nm) by a water-in-oil (w/o) microemulsion templating method.[13] Subsequently, size-controlled gold nanocatalysts (2.8 to 4.5 nm) inside the HSNs (yolk−shell type), Au@HSNs, were prepared.[14] They displayed high thermal stability and resistance to poisons in reaction solutions due to their shell barrier. Poison-resistant property, due to blocking of poisonous molecules in solution, was demonstrated for the reduction of nitrophenol.

When the silica shell of the yolk−shell nanoreactor is porous,[15,16] it would be highly desirable to further build a corking and uncorking mechanism onto the nanoreactor. The corking mechanism would be a switch for the smart reactor, which would be useful for applications. The size of Au NPs in Au@HSNs (at ∼3 nm) is in the catalytically interesting range; and we would like to apply it to the benchmark size-sensitive CO oxidation reaction. The nanocatalyst system needs to undergo high-temperature pretreatment to activate the gold NP. We will show that the size of gold NPs is very stable under the confinement of HSN. For the corking mechanism, we take advantage of the capillary condensation of water vapor in the mesopores of the shell to act as a reversible switch. Furthermore, water vapor is known to be a promoter for Au-catalyzed CO oxidation.[17] It will plug the reactor below a certain temperature T_p, and above T_p water vapor and reactants can enter the HSN giving an enhanced reaction rate. The concept of a vapor-switchable nanoreactor may be also applicable to other hollow sphere systems.[3] Because of the physical process of condensation and shell protection of the gold NP, the switch is reversible and stable over long time

Received: October 2, 2011
Accepted: November 10, 2011
Published: November 10, 2011

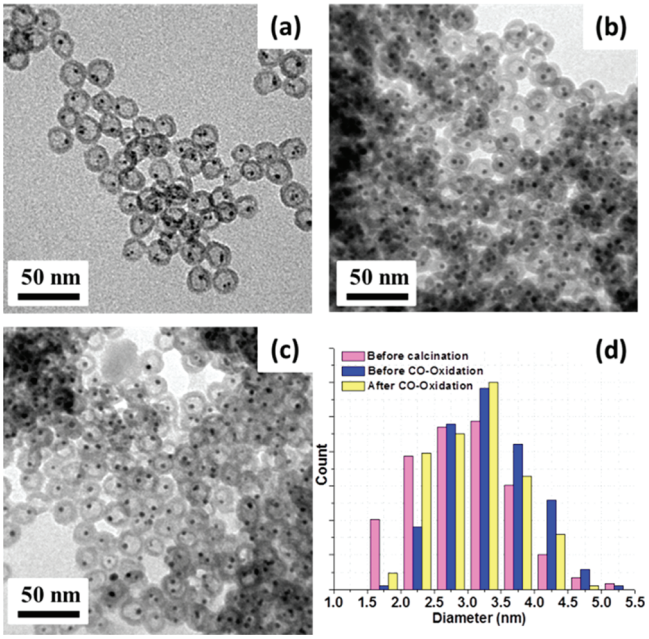

Figure 1. TEM images of Au@HSN (a) before calcination, (b) after calcination, and (c) after CO oxidation. (d) The size distributions of Au NPs at different stages.

periods as compared to other switching methods[18,19] in which aggregation of Au NPs is involved.

Herein, we used w/o reverse microemulsion to synthesize Au NPs encapsulated in HSNs (Au@HSNs). A microemulsion system with aqueous hydrogen tetrachloroaurate(III) as the water phase and cyclohexane as the oil phase was stabilized by surfactants. A mixture of tetraethyl orthosilicate (TEOS) and (3-aminopropyl)-triethoxysilane (APTS) ethanoic solution was added into the microemulsion, and ammonia hydroxide was added to the solution to initiate the hydrolysis.

After 36 h of aging, as-synthesized nanospheres were isolated from solution by centrifugation. Finally, $NaBH_4$ was added to reduce $[Au(Cl)_4]^-$ to Au NPs. Au@HSNs_C was obtained after calcination at 560 °C for 6 h. The gold content is 11.04%. Transmission electron microscopy (TEM) images and the size distributions of Au@HSNs before calcination and after reaction are shown in Figure 1. From the TEM images, the average size of gold NPs encapsulated in HSNs only grew slightly after calcination (from 2.91 ± 0.74 nm to 3.26 ± 0.66 nm). Furthermore, the size of the gold NPs did not significantly change after CO oxidation (from 3.26 ± 0.66 nm to 3.15 ± 0.67 nm). We see that the silica shell of Au@HSNs protected the gold NPs from sintering during calcination and CO oxidation. We also examined the nitrogen-adsorption isotherm for the two materials of the HSN after calcination, with or without loadings of gold. Both show large hysteresis of adsorption volume at $P/P_0 \sim 0.9$ (Figure S1, Supporting Information) due to enclosure of the large interior volume by the mesoporous silica shell. The pore volumes of the Au@HSN_C catalyst according to the nitrogen adsorption results is 0.53 cm^{-3} g^{-1}, of which a large fraction is contributed by intrasphere cavity. However, as explained in the Supporting Information, due to a forced closure of the hysteresis loop that originated from the tensile strength effect (TSE, a sudden evaporation due to tensile failure),[20] the pore size on the silica shell of the HSN cannot be determined from a nitrogen desorption curve.

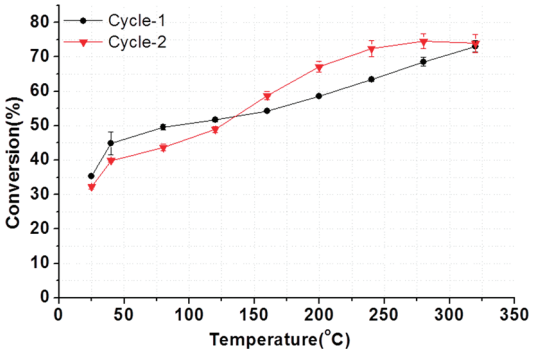

Figure 2. CO conversion for Au@HSNs_C (cycle-1) and for the catalyst stored for 3 months (cycle-2) with GHSV = 360 000 mL·g_{cat}^{-1}·h^{-1} ((1%CO/6%O_2/93%He) in a temperature range from 25 °C to 320 °C.

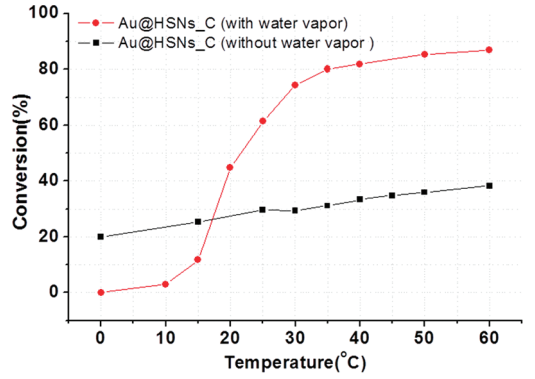

Figure 3. CO conversion of Au@HSNs_C with GHSV = 360 000 mL·g_{cat}^{-1}·h^{-1} (1%CO/6%O_2/93%He) under vapor and vapor-free conditions at a temperature range of 0−60 °C.

Before testing the CO oxidation, Au@HSNs_C was pretreated with H_2 at 600 °C for 30 min. We tested the reaction under a gas flow of 1% CO and 6% O_2 balanced with He. In Figure 2, the black curve shows the CO conversion as a function of reaction temperature. It increased with temperature up to 280 °C and then slightly declined. Notice that the conversion never reached 100% at high temperature. This is because we were deliberately using a very fast flow rate and a small amount of catalyst such that the gas hourly space velocity (GHSV) = 360 000 mL·g_{cat}^{-1}·h^{-1}. The reaction rate leveled at 280 °C and became limited by the rate of transport through the shell. After 3-month storage of the nanocatalyst under ambient conditions, the catalytic activity is tested again with the same pretreatment, and it retains almost the same stable activity as before (cycle-2 in Figure 2). In another long-time activity test of Au@HSNs_C with GHSV = 180 000 mL·g_{cat}^{-1}·h^{-1} (1%CO/6%O_2 /93%He) at room temperature, CO conversion remains constant (roughly at 60%) for 75 h (Figure S2). Moreover, when we decrease the oxygen content to 1%, over the temperature range of 25 °C to 320 °C, two runs separated by a 1 month period gave almost exactly the same conversion curve (Figure S3). These show that the Au@HSNs_C catalyst is very stable with the protection of the silica shell. The structure and activity of the nanocatalyst apparently survived after harsh treatment and long storage and reaction time. We also notice at the high T end that conversion did not reach 100%. This is probably due to the

dx.doi.org/10.1021/jz201336h |J. Phys. Chem. Lett. 2011, 2, 2984–2988

Scheme 1. Corking and Uncorking Mechanism by the Capillary Condensation of Water Vapor

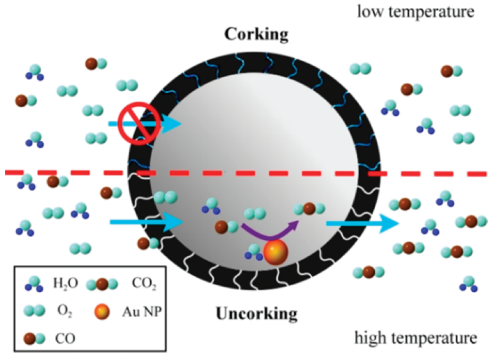

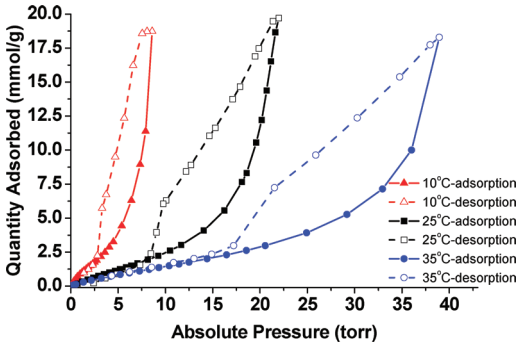

Figure 4. Water adsorption−desorption isotherms of Au@HSNs _C at different temperatures: (−▲−) 10 °C; (−■−) 25 °C; (−●−) 35 °C.

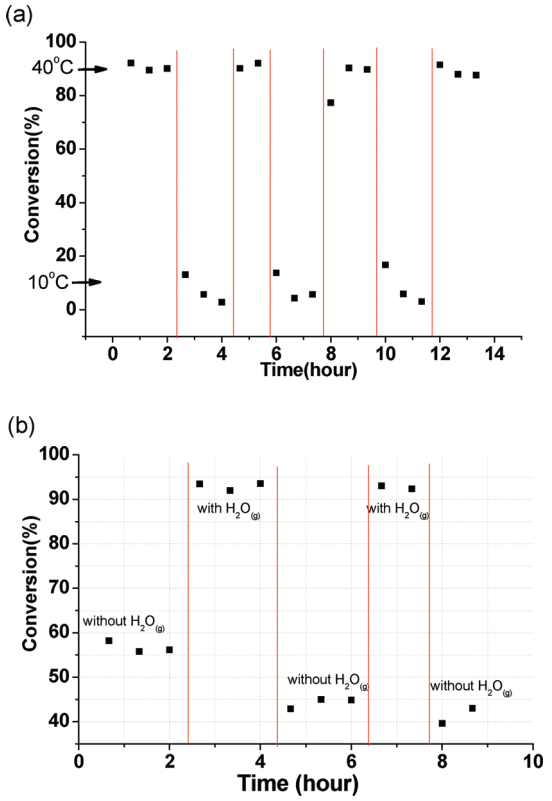

Figure 5. (a) CO conversion of a catalyst at 40 °C and 10 °C under water vapor atmosphere with GHSV = 360 000 mL·g_{cat}^{-1}·h^{-1} (1% CO/6% O_2/93%He). (b) CO conversion of Au@HSNs_C with GHSV = 360 000 mL·g_{cat}^{-1}·h^{-1} (1%CO/6%O_2/93%He) under vapor and vapor-free atmospheres at 40 °C.

diffusion-limited barrier across the shell at such a very high GHSV (as the reaction order in Figure S4 indicates).

The absolute reaction rate was evaluated at low conversion; it is 0.512 mol·g_{Au}^{-1}·h^{-1} at 25 °C and 0.729 mol·g_{Au}^{-1}·h^{-1} at 80 °C, better than some of the best Au nanocatalysts on silica in the literature.[21−24] For a detailed comparison with the literature, see Table S1.

Next, we examine the catalytic activity in the presence of moisture. Haruta and co-workers[17] previously reported that moisture had a promotional effect on the catalytic activity of silica-supported gold NPs. A proper concentration of moisture could enhance the catalytic activity of the CO oxidation reaction. Thus, we studied the CO oxidation reaction of Au@HSNs_C under moisture atmosphere. Figure 3 gives CO conversion as catalyzed by Au@HSNs_C at GHSV = 360 000 mL·g_{cat}^{-1}·h^{-1} (1%CO/6%O_2/93%He) with either 25 °C-saturated H_2O vapor or water-free atmosphere. From Figure 3, one first sees a slow increase of rate versus T over the temperature range of 0 °C to 60 °C at dry conditions. However, with water vapor injected, one can see a sharp increase of CO conversion from 0 to 85% as the temperature was increased from 10 °C to 40 °C. The catalytic activity seemed to be inhibited when the temperature was lower than 25 °C, but the catalytic activity was enhanced 3 times compared with vapor-free conditions when the temperature was higher than 25 °C.

We propose a model to explain the switching phenomena as shown in Scheme 1. At a temperature above 25 °C, the pores on the silica shell of the Au@HSNs_C catalyst were open. Thus, not only could the reactant gas contact the gold catalyst, but also the water vapor promoted the production of CO_2. When the temperature was below 25 °C, the moisture condensed in the pores of the silica shell, blocked the channel, and kept the reactant from reaching gold NPs. The pores on the silica shell were blocked, and no CO_2 molecules could be produced through the catalysts.

To support the corking/uncorking mechanism in Scheme 1, we measured the adsorption isotherm of water vapor at 10, 25, and 35 °C. Figure 4 shows the water adsorption isotherms for the Au@HSN_C catalyst. At all three temperatures, large hysteresis behavior can be observed. This unequivocally confirms that the mesopores on the shell of the hollow nanosphere block desorption of the large interior volume. The adsorption curves at different temperatures show that the condensation of moisture occurred at lower pressure when the temperature was low. The intersections of adsorption and desorption curves are at 9.0, 24.0, and 42.0 Torr, respectively. In terms of relative pressure P/P_0, the hysteresis closure is between 0.4 and 0.45, also indicating a TSE phenomenon. We also note that the saturation adsorption volume measured by water vapor near room temperature is roughly 0.36 cm^{-3} g^{-1}, which is somewhat smaller than that measured by nitrogen adsorption at 77 K (0.54 cm^{-3} g^{-1}), which should have more complete condensation.

We plot the isotherms in absolute pressure (torr) instead of relative to saturation in order to see the condensation of water vapor at lower temperature. Hence, the surface pores of the catalyst were blocked due to capillary condensation of moisture at 10 °C when the reaction system was introduced with water

dx.doi.org/10.1021/jz201336h |J. Phys. Chem. Lett. 2011, 2, 2984–2988

vapor at 24 Torr (25 °C saturated water vapor). On the other hand, capillary evaporation occurs at 35 °C, as the reactant gas could contact the catalysts without obstruction. Thus, the designed experiments show that one could just use the near-saturation moisture to turn on/off the CO oxidation reaction inside the Au@HSNs_C nanoreactor. In Figure 5a, one sees that the CO conversion was enhanced by moisture at 40 °C and inhibited at 10 °C. Moreover, the CO oxidation could be rapidly turned on and off in an almost instant manner as the temperature jumped between the two temperatures. The switch was quite reversible. In addition, the switching could be executed by the swing of water vapor. Figure 5b illustrates CO conversion under the switching between water vapor and vapor-free conditions at 40 °C. The CO conversion was enhanced in the presence of moisture and dropped to a low level in the absence of moisture. However, the changes of conversion upon switching are not as big as the one in Figure 5a. Hence, either temperature or water vapor switching could control the catalytic activity of CO oxidation. For comparison, we also measured the corking/uncorking effect of another similar system Au@SBA-15 under quite similar conditions, as shown in the Supporting Information. Figure S5 shows milder switching action, and Figure S6 also shows switching of conversion swinging between 40 and 10 °C with much smaller changes in conversion due to the larger pore in SBA-15 and incomplete enclosure of all the Au catalysts.

Above the pore-opening temperature, the reaction is not only helped by contact of reactants with Au NP inside the yolk−shell nanoreactor, but is also promoted by the contact of water with catalyst. However, water gas shift (WGS) reaction did not occur in the low temperature range in Figure 3. We never detected the production of hydrogen. Recently, Mullins and co-workers[25] studied water-enhanced low-temperature CO oxidation and concluded that the promotional effect is due to Au-adsorbed water and oxygen to form two OH molecules, which react with CO to produce CO_2 and H_2O. No WGS was observed in the low temperature range in which we worked.

In conclusion, we have presented a stable reactor containing gold NPs of well-controlled size for catalytic oxidation of CO. Its activities are very stable over long-term storage or high-temperature treatment. The reactor can be reversibly switched to different levels by a small temperature jump or water vapor. The stimulus−response reactor, based on mesoporous silica, is more stable as compared to other types of cage reactors based on synthetic organic or biological building blocks.[26]

■ ASSOCIATED CONTENT

Ⓢ Supporting Information. Experimental procedures for the synthesis of the catalysts, measurement of activities, nitrogen/water adsorptions, long time stability tests, and reaction order and reaction rate comparison with the literature. This material is available free of charge via the Internet at http://pubs.acs.org.

■ AUTHOR INFORMATION

Corresponding Author
*E-mail: cymou@ntu.edu.tw.

■ ACKNOWLEDGMENT

We are very thankful to Dr. Yann Hung for discussions and the National Nanotechnology Project of National Science Council (Taiwan) for financial support.

■ REFERENCES

(1) Centi, G.; Perathoner, S. Creating and Mastering Nano-objects to Design Advanced Catalytic Materials. *Coordin. Chem. Rev.* **2011**, *255*, 1480–1498.

(2) Ma, Z.; Dai, S. Development of Novel Supported Gold Catalysts: A Materials Perspective. *Nano Res.* **2011**, *4*, 3–32.

(3) Zhu, K.; Wang, D. G.; Liu, J. Self-Assembled Materials for Catalysis. *Nano Res.* **2009**, *2*, 1–29.

(4) Cao, A.; Lu, R.; Veser, G. Stabilizing Metal Nanoparticles for Heterogeneous Catalysis. *Phys. Chem. Chem. Phys.* **2010**, *12*, 13499–13510.

(5) Ma, Z.; Dai, S. Design of Novel Structured Gold Nanocatalysts. *ACS Catal.* **2011**, *1*, 805–818.

(6) Laoufi, I.; Saint-Lager, M. C.; Lazzari, R.; Jupille, J.; Robach, O.; Garaudee, S.; Cabailh, G.; Dolle, P.; Cruguel, H.; Bailly, A. Size and Catalytic Activity of Supported Gold Nanoparticles: An in Operando Study During CO Oxidation. *J. Phys. Chem. C* **2011**, *115*, 4673–4679.

(7) Chen, C.; Nan, C. Y.; Wang, D. S.; Su, Q. A.; Duan, H. H.; Liu, X. W.; Zhang, L. S.; Chu, D. R.; Song, W. G.; Peng, Q.; Li, Y. D. Mesoporous Multicomponent Nanocomposite Colloidal Spheres: Ideal High-Temperature Stable Model Catalysts. *Angew. Chem., Int. Ed.* **2011**, *50*, 3725–3729.

(8) Zhao, M. Q.; Zhang, Q.; Zhang, W.; Huang, J. Q.; Zhang, Y. H.; Su, D. S.; Wei, F. Embedded High Density Metal Nanoparticles with Extraordinary Thermal Stability Derived from Guest−Host Mediated Layered Double Hydroxides. *J. Am. Chem. Soc.* **2010**, *132*, 14739–14741.

(9) Lou, X. W.; Archer, L. A.; Yang, Z. C. Hollow Micro-/Nanostructures: Synthesis and Applications. *Adv. Mater.* **2008**, *20*, 3987–4019.

(10) Zhao, Y.; Jiang, L. Hollow Micro/Nanomaterials with Multilevel Interior Structures. *Adv. Mater.* **2009**, *21*, 3621–3638.

(11) Arnal, P. M.; Comotti, M.; Schuth, F. High-Temperature-Stable Catalysts by Hollow Sphere Encapsulation. *Angew. Chem., Int. Ed.* **2006**, *45*, 8224–8227.

(12) Chen, H. M.; Hu, T.; Zhang, X. M.; Huo, K. F.; Chu, P. K.; He, J. H. One-Step Synthesis of Monodisperse and Hierarchically Mesostructured Silica Particles with a Thin Shell. *Langmuir* **2010**, *26*, 13556–13563.

(13) Lin, Y. S.; Wu, S. H.; Tseng, C. T.; Hung, Y.; Chang, C.; Mou, C. Y. Synthesis of Hollow Silica Nanospheres with a Microemulsion as the Template. *Chem. Commun.* **2009**, 3542–3544.

(14) Wu, S. H.; Tseng, C. T.; Lin, Y. S.; Lin, C. H.; Hung, Y.; Mou, C. Y. Catalytic Nano-rattle of Au@Hollow Silica: Towards a Poison-Resistant Nanocatalyst. *J. Mater. Chem.* **2011**, *21*, 789–794.

(15) Wang, J. G.; Li, F.; Zhou, H. J.; Sun, P. C.; Ding, D. T.; Chen, T. H. Silica Hollow Spheres with Ordered and Radially Oriented Amino-Functionalized Mesochannels. *Chem. Mater.* **2009**, *21*, 612–620.

(16) Wang, Y.; Su, F. B.; Lee, J. Y.; Zhao, X. S. Crystalline Carbon Hollow Spheres, Crystalline Carbon−SnO_2 Hollow Spheres, and Crystalline SnO_2 Hollow Spheres: Synthesis and Performance in Reversible Li-Ion Storage. *Chem. Mater.* **2006**, *18*, 1347–1353.

(17) Date, M.; Okumura, M.; Tsubota, S.; Haruta, M. Vital Role of Moisture in the Catalytic Activity of Supported Gold Nanoparticles. *Angew. Chem., Int. Ed.* **2004**, *43*, 2129–2132.

(18) Wei, Y. H.; Han, S. B.; Kim, J.; Soh, S. L.; Grzybowski, B. A. Photoswitchable Catalysis Mediated by Dynamic Aggregation of Nanoparticles. *J. Am. Chem. Soc.* **2010**, *132*, 11018–11020.

(19) Lv, W. P.; Wang, Y.; Feng, W. Q.; Qi, J. J.; Zhang, G. L.; Zhang, F. B.; Fan, X. B. Robust and Smart Gold Nanoparticles: One-Step Synthesis, Tunable Optical Property, and Switchable Catalytic Activity. *J. Mater. Chem.* **2011**, *21*, 6173–6178.

(20) Groen, J. C.; Peffer, L. A. A.; Perez-Ramirez, J. Pore Size Determination in Modified Micro- and Mesoporous Materials. Pitfalls and Limitations in Gas Adsorption Data Analysis. *Microporous Mesoporous Mater.* **2003**, *60*, 1–17.

(21) Yen, C. W.; Lin, M. L.; Wang, A. Q.; Chen, S. A.; Chen, J. M.; Mou, C. Y. CO Oxidation Catalyzed by Au−Ag Bimetallic Nanoparticles Supported in Mesoporous Silica. *J. Phys. Chem. C* **2009**, *113*, 17831–17839.

(22) Budroni, G.; Corma, A. Gold-Organic−Inorganic High-Surface-Area Materials as Precursors of Highly Active Catalysts. *Angew. Chem., Int. Ed.* **2006**, *45*, 3328–3331.

(23) Liu, X. Y.; Wang, A. Q.; Wang, X. D.; Mou, C. Y.; Zhang, T. Au−Cu Alloy Nanoparticles Confined in SBA-15 as a Highly Efficient Catalyst for CO Oxidation. *Chem. Commun.* **2008**, 3187–3189.

(24) Chiang, C. W.; Wang, A. Q.; Wan, B. Z.; Mou, C. Y. High Catalytic Activity for CO Oxidation of Gold Nanoparticles Confined in Acidic Support Al-SBA-15 at Low Temperatures. *J. Phys. Chem. B* **2005**, *109*, 18042–18047.

(25) Ojifinni, R. A.; Froemming, N. S.; Gong, J.; Pan, M.; Kim, T. S.; White, J. M.; Henkelman, G.; Mullins, C. B. Water-Enhanced Low-Temperature CO Oxidation and Isotope Effects on Atomic Oxygen-Covered Au(111). *J. Am. Chem. Soc.* **2008**, *130*, 6801–6812.

(26) Kim, K. T.; Meeuwissen, S. A.; Nolte, R. J. M.; van Hest, J. C. M. Smart Nanocontainers and Nanoreactors. *Nanoscale* **2010**, *2*, 844–858.